Detailed metabolic phenotyping of four tissue specific Cas9 transgenic mouse lines

Simon T. Bond[1,2,3], Aowen Zhuang[1,2,3], Christine Yang[1], Eleanor A.M. Gould[1], Tim Sikora[1],

Yingying Liu[1], Ying Fu[1], Kevin I. Watt[4], Yanie Tan[1], Helen Kiriazis[1], Graeme I. Lancaster[1],

Paul Gregorevic[4,5,6], Darren C. Henstridge[1,7], Julie R. McMullen[1,2,3,8], Peter J. Meikle[1,2,3],

Anna C. Calkin[1,2,3] & Brian G. Drew[1,2,3]*

1. Baker Heart & Diabetes Institute, Melbourne, Australia, 3004.

2. Baker Department of Cardiometabolic Health, The University of Melbourne, Melbourne, Australia,

3. Central Clinical School, Monash University, Melbourne, Australia, 3004

4. Centre for Muscle Research, Department of Anatomy and Physiology, School of Biomedical Sciences, The University of Melbourne, Australia

5. Department of Biochemistry and Molecular Biology, Monash University, Clayton, Australia

6. Department of Neurology, The University of Washington School of Medicine, Seattle, WA, USA

7. College of Health and Medicine, School of Health Sciences, University of Tasmania, Launceston, Australia.

8. Department of Physiology, Anatomy and Microbiology, La Trobe University, Bundoora, Australia

*Author for correspondence: brian.drew@baker.edu.au.

Abstract

CRISPR/Cas9 technology has revolutionized gene editing and fast tracked our capacity to manipulate genes of interest for the benefit of both research and therapeutic applications. Whilst many advances have, and continue to be made in this area, perhaps the most utilized technology to date has been the generation of knockout cells, tissues and animals by taking advantage of Cas9 function to promote indels in precise locations in the genome. Whilst the advantages of this technology are many fold, some questions still remain regarding the effects that long term expression of foreign proteins such as Cas9, have on mammalian cell function. Several studies have proposed that chronic overexpression of Cas9, with or without its accompanying guide RNAs, may have deleterious effects on cell function and health. This is of particular concern when applying this technology in vivo, where chronic expression of Cas9 in tissues of interest may promote disease-like phenotypes and thus confound the investigation of the effects of the gene of interest. Although these concerns remain valid, no study to our knowledge has yet to demonstrate this directly. Thus, in this study we used the lox-stop-lox (LSL) spCas9 ROSA26 transgenic (Tg) mouse line to generate four tissue-specific Cas9-Tg models with expression in the heart, liver, skeletal muscle and adipose tissue. We performed comprehensive phenotyping of these mice up to 20-weeks of age and subsequently performed molecular analysis of their organs. We demonstrated that Cas9 expression in these tissues had no detrimental effect on whole body health of the animals, nor did it induce any tissue-specific effects on energy metabolism, liver health, inflammation, fibrosis, heart function or muscle mass. Thus, our data suggests that these models are suitable for studying the tissue specific effects of gene deletion using the LSL-Cas9-Tg model, and that phenotypes observed utilizing these models can be confidently interpreted as being gene specific, and not confounded by the chronic overexpression of Cas9.

Introduction

51   Since the discovery and proven utility of CRISPR/Cas9 based gene editing technologies,

52   there has been a proliferation of applications that take advantage of this ground-breaking

53   technology. Whilst the potential for this relatively simple but precise, genetic manipulation

54   tool is obvious, the speed at which the field is developing often means that subtle off-target

55   and deleterious effects of such an approach can be overlooked. Studies over the past 5 years

56   have demonstrated that each system requires important optimization to ensure accurate gene

57   editing, whilst minimizing off-target editing and potential toxicity induced by the

58   introduction of foreign genetic machinery (Broeders et al., 2020; Molla and Yang, 2019).

59

60   A major advantage of CRISPR based editing in the pre-clinical biomedical arena is the rapid

61   development of animal models that harbor global gene deletions or conditional targeting of

62   alleles. These models historically took 2-3 years to generate, where now a global deletion

63   model using CRISPR can take 3 months or less to generate (Singh et al., 2015). Moreover,

64   CRISPR overcomes the need to generate one mouse model per gene of interest, as is the case

65   with floxed alleles. Indeed, by over-expressing Cas9 globally in mice, or in a tissue specific

66   manner, one can generate a model where almost any gene can be manipulated simply by

67   introducing a guide RNA that targets your gene of interest. This flexibility of manipulation

68   has made it feasible to use one mouse model, or even an existing disease model, to study the

69   effect of manipulating one or many genes in combination.

70

71   One such model developed is the lox-STOP-lox spCas9-transgenic (LSL-spCas9Tg) mouse

72   (Platt et al., 2014). This model harbors the spCas9 gene at the ROSA26 locus, but is silenced

73   in the basal state by commonly applied repressor elements. By flanking the repressor or

74   "STOP" element with loxP sites, the construct becomes inducible in the presence of Cre-

75   recombinase. This model has been used by a number of groups to demonstrate robust Cas9

76   expression induced by Cre-recombinase, and subsequent CRISPR mediated gene editing

77   upon the administration of a guide RNA (Laidlaw et al., 2020; Shamsi et al., 2020; Zhu et al.,

78   2020).

79

80   One concern with such an approach is whether chronic expression of the foreign CRISPR

81   machinery mediates phenotypic effects *per se* (Broeders et al., 2020). To this end, we have

82   successfully developed four tissue-specific Cas9 transgenic mouse models that include key

83   tissues of interest in the metabolism field (skeletal muscle, liver, adipose tissue and heart).

84   We phenotyped these animals for readouts of whole body metabolism, adiposity, glucose

85   tolerance, toxicity and cardiac function, and demonstrated that none of the models were

86   impacted by the chronic (~12 weeks) presence of Cas9. These findings provide important and

87   much needed confidence for researchers who wish to use these mouse models in the future,

88   who can now confidently ascribe any observed metabolic phenotype to their gene of interest,

89   and not to underlying unwanted side effects of the model itself.

90   **Results**

91   **Tissue Specific and Inducible Expression of Cas9 in four mouse models.**

92   To generate tissue specific Cas9 transgenic mice, we crossed the LSL-spCas9 Tg mouse

93   (Platt et al., 2014) with four different tissue specific Cre-recombinase transgenic mouse lines.

94   Three of these models (ACTA1-Cre, AdipoQ-Cre and MHCalpha-Cre) were tamoxifen

95   inducible via the use of Cre-recombinase that was fused to the modified estrogen receptor

96   (mER), often referred to as ERT2. The other model (albumin-Cre) was constitutively active

97   and expressed from the albumin promoter (Alb-Cre). These breeding strategies resulted in

98   four separate mouse models with an expected tissue specific expression of Cas9 in liver

99   (Albumin), heart (MHC-alpha), skeletal muscle (ACTA1), and adipose tissue (AdipoQ),

100 (**Figure 1A**).

101

102 Because three of the Cre-models were inducible (with tamoxifen), we administered tamoxifen

103 or vehicle (oil) using specific regimens for each model (see methods) between 6-8 weeks of

104 age, then allowed 2 weeks for maximal gene expression before any phenotyping was

105 performed. For the inducible models, we studied four cohorts of mice per model, which

106 included: Cre+OIL (Cre-inactive), Cas9+Cre+OIL (Cas9+Cre-inactive), Cre+Tamoxifen

107 (Cre-active) and Cas9+Cre+Tamoxifen (Cas9+Cre-active) mice. For the constitutively active

108 Albumin-Cre model, there was no oil/tamoxifen treatment so there were only two cohorts;

109 Cre-active and Cas9+Cre-active.

110

111 To characterize the different models, we performed phenotyping that included assessment of

112 body weight, fat mass and lean mass by EchoMRI, and glucose tolerance tests (GTTs) which

113 were performed at various times for different models over the subsequent 12 weeks. We also

5

114   performed some model specific phenotyping, including echocardiography of the MHC-alpha

115   model to analyze heart function.

116

117   At the completion of each study (mice up to approximately 20-22 weeks of age), tissues were

118   collected, processed and analyzed to first confirm that each model displayed the expected

119   expression profiles. Using qPCR analysis, we demonstrated that each model exhibited tissue

120   specific Cre-recombinase expression, with robust expression in the expected tissue, but no

121   detected expression in other tissues (**Figure 1B**). Importantly, we also demonstrate using

122   qPCR that Cas9 expression was tissue specific, and that this expression was dependent on

123   both Cre-expression and the administration of tamoxifen in the inducible models. As a

124   secondary confirmation we also determined the abundance of GFP by qPCR, which is co-

125   expressed from the same transgene cassette as Cas9, but is independently processed by the

126   ribosome (i.e. not tagged to Cas9). We demonstrated that both Cas9 and GFP exhibited the

127   expected tissue specific expression profiles including liver (**Figure 1C**), heart (**Figure 1D**),

128   muscle (**Figure 1E**) and white adipose tissue (WAT, **Figure 1F**). The level of Cas9 induction

129   varied slightly across the lines, which is likely a reflection of local transcriptional machinery,

130   number of cells per unit of tissue, and the differential activity of Cre-recombinase in each

131   tissue.

132

133   **Tissue Specific Expression of Cre-Recombinase, Cas9 and GFP does not Impact Animal**

134   **Body Weight or Tissue Weights.**

135   Upon demonstrating that each model expressed Cas9 in a tissue specific manner, we next

136   sought to test previously raised concerns that chronic over-expression of "foreign" enzymes

137   such as Cre and Cas9 in metabolic tissues, might lead to phenotypic differences in animal

138   growth and development. A simple way of testing for toxicity or growth inhibition is to

139   compare body weight and individual tissue weights from each model at study end. We

140   demonstrate that body weights for each model were comparable between cohorts at the time

141   of cull, with no significant differences in body weight, whether they were expressing Cre,

142   Cas9, or if they had been treated with tamoxifen/oil (**Figure 2A**). Moreover, assessment of

143   liver, WAT, Muscle (*Tibialis anterior*; TA) and heart weights at the time of cull,

144   demonstrated no difference in the weight of any of these tissue between the various groups

145   within each model (**Figures 2B-2E**).

146

147   **Tissue Specific Expression of Cre-Recombinase, Cas9 and GFP does not Alter**

148   **Molecular or Physiological Readouts of Tissue Function.**

149   Whilst it was important to demonstrate that there was no effect of Cas9 expression on gross

150   tissue weights or animal growth, we also sought to investigate whether tissue specific

151   pathways were being impacted by chronic over expression of Cas9 in each tissue. Therefore,

152   we performed a series of analyzes on each tissue to investigate these parameters, utilizing

153   qPCR, histology and functional assessment.

154

155   In the liver specific Cas9 model (Alb-Cre), we used qPCR to analyze the expression of genes

156   that were representative of pathways that provided insight into the health and activity of the

157   liver. These included *Col1a2* and *Vim* as markers of fibrosis, *Chop* for ER stress, *Plin2* for

158   lipid storage and *Tnfa* and *Il1b* for inflammation (**Figure 3A**). We demonstrated that none of

159   these genes were differentially expressed in mice with livers expressing Cas9 compared to

160   control livers, indicating that the expression of Cas9 in the liver was not impacting on liver

161   inflammation, fibrosis or lipid handling. Moreover, representative histological sections

162   stained with hematoxylin and eosin (H&E) demonstrated no gross changes in liver

163   morphology (**Figure 3B**).

7

164

165   In the heart specific Cas9 model (MHCa-Cre), we used qPCR to measure pathways in the

166   heart that are indicative of cardiac health and function. These included classic molecular

167   markers of heart failure including Atrial Natriuretic Peptide (ANP) (*Nppa)* and B-type

168   Natriuretic Peptide (BNP) (*Nppb*) as well as αMHC (*Myh6*) and βMHC (*Myh7*). We also

169   measured a marker of fibrosis (*Col1a1*) and a marker of cardiac contractile function via the

170   sarcoplasmic reticulum /endoplasmic reticulum Ca2+ ATPase 2a (SERCA; *tp2a2*) (**Figure**

171   **3C**). We demonstrate that were no differences in the expression of any of these markers in

172   the left ventricle (LV) across the four groups of mice, implying that these pathways were not

173   altered by the expression of Cas9 (or Cre-recombinase). This was supported by data

174   demonstrating that the weight of the whole heart and the different regions of the heart from

175   these mice including; atria, LV and right ventricle (RV), were also not different between

176   groups (**Figure 3D**). Consistently, the lung weights, spleen weight and kidney weight (which

177   are useful readouts of health in cardiac models) were all comparable across groups

178   demonstrating no peripheral effects of cardiac specific overexpression of Cas9. Lastly, we

179   assessed heart function in these mice using echocardiography. We demonstrated that at

180   comparable heart rates (HR), under anesthesia there were no differences in fractional

181   shortening (FS%) – a measure of systolic function, between the four groups (**Figure 3E**).

182   Thus, collectively these data demonstrate that overexpression of Cas9 in cardiomyocytes has

183   no impact on heart health and function.

184

185   Specific phenotyping of the muscle specific Cas9 model (ACTA1-Cre) was also performed

186   using qPCR. We measured the expression of muscle specific genes that are known readouts

187   of muscle development and growth in the TA muscle. These included myogenic transcription

188   factors *Myod, Myog* and *Mef2c*, as well as the pro-fusion protein myomaker (*Tmem8c*) and

8

189   mature muscle marker *Mck* (**Figure 3F**). As with our previous models, we demonstrated no

190   difference in the expression of these genes between the four groups of mice, indicating that

191   there were no major differences in the growth and function of adult skeletal muscle in the

192   presence of Cas9 expression. In support of this data, using EchoMRI we demonstrated that

193   there was no difference in lean muscle mass across the four groups, at any time point

194   throughout the study period (**Figure 3G**). Finally, histological analyzes of TA muscle

195   sections using H&E staining, indicated that there were no major morphological differences in

196   the muscle structure between Cas9 positive and Cas9 negative mice (**Figure 3H**).

197   Collectively, these data indicate that Cas9 expression in skeletal muscle has no impact on

198   muscle health and maturation.

199

200   The final model we characterized was the adipose-specific Cas9 mouse (AdipoQ-Cre). As

201   with previous models, using qPCR we demonstrated that there was no major difference in the

202   expression of genes related to adipocyte differentiation and health in WAT, including the

203   adipogenic transcription factors PPARgamma (*Pparg*) and C/EBPalpha (*Cebpa*), the lipid

204   transporter *Cd36*, inflammatory markers *Tnfa* and *Il1b*, and the browning marker *Ucp1*

205   (**Figure 3I**). Moreover, using EchoMRI we demonstrated that there was no difference in fat

206   mass between the four groups in this AdipoQ-Cre model at any time point throughout the

207   study period (**Figure 3J**). Finally, histological assessment of WAT sections using H&E

208   staining, indicated that there were no major morphological differences in adipocyte size or

209   structure between Cas9 positive and Cas9 negative mice (**Figure 3K**). Collectively, these

210   data indicate that Cas9 expression in adipose tissue has no impact on WAT health and

211   development.

212

213 **Tissue Specific Expression of Cre-Recombinase, Cas9 and GFP does not Alter Whole**

214 **Body Glucose Homeostasis.**

215 Given that many groups which study metabolism have an interest in glucose homeostasis and

216 how it relates to tissues such as liver, adipose, skeletal muscle and the heart, we sought to

217 determine if the expression of Cas9 in these tissue led to any changes in whole body glucose

218 handling. To investigate this, we performed fasting blood glucose measurements and oral

219 glucose tolerance tests on all groups and models within the final two weeks of the study

220 period. We demonstrated that there was no difference in fasting blood glucose levels between

221 Cas9 positive and Cas9 negative mice in each of the four tissue specific mouse models

222 (**Figures 4A, 4D, 4G and 4J**). In order to test the glucose tolerance of these models, we

223 challenged each cohort with a standardized oral dose of glucose (2mg/kg lean mass), and

224 subsequently measured their blood glucose concentration over two hours in an oral glucose

225 tolerance test (oGTT). We demonstrated that all groups and models showed a peak glucose

226 concentration of approximately 18-20mmol/L at 15 minutes post glucose delivery, which

227 mostly returned to baseline by 60 minutes after delivery of the glucose bolus (**Figures 4B,**

228 **4E, 4H and 4K**). We also demonstrated that there was no difference in the clearance of

229 glucose across any of the groups and in each of the models, indicating that there was no

230 difference in the glucose tolerance of these animals. This is further demonstrated

231 quantitatively by assessing the 90 minute cumulative area under the curve (AUC) for the

232 tolerance test (**Figures 4C, 4F, 4I and 4L**), confirming that there was no difference in

233 glucose tolerance between the groups in each tissue specific Cas9 model.

234

235 Collectively, the data presented above demonstrates that long term overexpression of Cas9 in

236 four different tissue specific models, does not lead to any effects on body weight, tissue

237 weight, the expression of markers of pathological pathways, or readouts of whole body

10

238 glucose metabolism. These findings provide an important foundation for future studies that

239 wish to use the LSL-Cas9 mouse model to study their gene of interest, and affords confidence

240 to researchers that metabolic phenotypes they measure are unlikely to be impacted by the

241 chronic over expression of Cas9 or Cre-recombinase in these models.

242 **Discussion**

243 The discovery and implementation of CRISPR Cas9 as a gene editing tool has far reaching

244 implications for furthering knowledge gain in biomedical science. The flexibility and

245 comparatively simple execution of this technology means it can be utilized by most research

246 laboratories around the world, accelerating the opportunity for discovery by several fold over

247 existing technologies. Whilst CRISPR Cas9 has indeed been adopted quickly and efficiently

248 by the scientific community, this has often been accomplished without due consideration for

249 the potential negative effects on metabolic readouts that might arise from such

250 methodologies, particularly if appropriate optimisation has not been performed. Many studies

251 have shown that spurious gene editing can occur in the setting of chronic, high level

252 expression of Cas9 (Hendel et al., 2015) and their accompanying single guide RNAs

253 (sgRNAs) (Fu et al., 2013; Link et al., 2018), whilst others have expressed concern over the

254 impacts of long term exogenous expression of CRISPR machinery (Cas9/sgRNAs), causing

255 unwanted effects on target cells (Charlesworth et al., 2019; Enache et al., 2020). Such

256 unwanted effects on targets cells would be particularly concerning in the in vivo setting,

257 where even minor disruptions to tissue function over many months has the potential to

258 substantially impact on animal health and disease risk. Unfortunately, the impact of these

259 unwanted effects is mostly unknown at this point, and is difficult to predict without

260 performing the experiments directly. This is likely time consuming and laborious, and thus

261 these important "control group comparisons" are often the first experiments to be overlooked

262 when designing new CRISPR editing experiments.

263

264 With regard to in vivo CRISPR editing, the generation of the inducible spCas9 transgenic

265 mouse (LSL-spCas9Tg) by Zhang and colleagues has been an important tool to enable tissue

266 and temporal specific Cas9 expression in mice (Platt et al., 2014). This model has been used

267   in several labs around the world to successfully delete genes of interest, most commonly in

268   myeloid or neuronal cell lineages (Laidlaw et al., 2020; Shamsi et al., 2020; Zhu et al., 2020).

269   Whilst there are obvious advantages to using this LSL-spCas9Tg mouse model, it is less

270   obvious what the potential disadvantages are - if any do exist. This is particularly true when

271   generating tissue specific Cas9 models for the first time, as there would be no data available

272   as to whether chronic Cas9 overexpression will impact the tissue of interest and the whole

273   body phenotypes of interest.

274

275   Given our group has a major interest in metabolism and the organs that regulate whole body

276   energy status, we are constantly performing studies in pertinent metabolic tissues such as the

277   liver, muscle, adipose and heart. Unfortunately, to date, few studies have performed in vivo

278   CRISPR editing in these tissues using the LSL-spCas9Tg mouse, and thus it is unclear as to

279   whether this model would be suitable for investigating CRISPR-mediated gene deletion in the

280   aforementioned tissues, without the risk of unwanted side effects due to chronic Cas9

281   overexpression.

282

283   We thus generated liver-, muscle-, adipose- and heart-specific Cas9 expressing mice using

284   the LSL-Cas9Tg model, and demonstrated that these four models appear to be unaffected by

285   the chronic expression of Cas9 and/or Cre-recombinase. We performed comprehensive

286   metabolic phenotyping of all four lines including body composition, glucose tolerance,

287   molecular and biochmical measurements, and functional readouts on various tissues. These

288   analyses demonstrated clear tissue specificity of Cas9 expression, driven by temporal

289   activation of Cre-recombinase using tamoxifen in all three of the inducible lines (muscle,

290   adipose and heart), as well as the constitutive albumin (liver) line. Importantly, we were

13

291   unable to detect any deleterious effects on metabolic pathways, morphology of tissues, body

292   composition or glucose tolerance in any lines over-expressing Cas9, supporting the notion

293   that there is no negative impact of chronic Cas9 expression in these tissues. Moreover,

294   echocardiography also demonstrated no impact on systolic heart function in cardiac-specific

295   Cas9 expressing mice after 20 weeks of induction, providing evidence that heart function in

296   these mice was not affected by chronic Cas9 expression.

297

298   In summary, we provide critical evidence that the metabolism and general health of four

299   different metabolic tissue specific mouse lines are unaffected by the chronic expression of

300   Cas9. These findings provide confidence for researchers moving forward, who wish to use

301   these Cas9 mouse models to manipulate the expression of genes in these particular tissues.

302   The minimal impact of Cas9 in these studies will likely reduce the need for future studies to

303   perform specific controls groups, reducing animal numbers and sparing expensive resources.

304   Our data will also provide confidence that observed phenotypes related to gene deletions in

305   these models in future studies, are likely to be specific to the gene of interest rather than

306   being related to the chronic over-expression of Cas9. Thus these findings provide an

307   important resource for the research community.

308

309

310

Methods

Generation of Tissue Specific Cas9 Animal Models

All animal experiments were approved by the Alfred Research Alliance (ARA) Animal Ethics committee (E/1756/2017/B) and performed in accordance with the research guidelines of the National Health and Medical Research Council of Australia. Tissue specific expression of Cas9 was achieved using the Cre-Lox system, where Cre-recombinase was used to remove the "STOP" sequence from the lox-stop-lox (LSL) cassette separating the promoter and Cas9 genes in the mouse described by Zhang et al (Platt et al., 2014). The four different mouse lines were generated by crossing the LSL-spCas9-Tg mouse with either the Albumin-Cre, ACTA1-Cre-ERT2, AdipoQ-Cre-ERT2 or MHCalpha-Cre-ERT2 mice. All mice were on a C57BL/6J background and are available from Jackson Laboratories. We generated two cohorts of n=8-10 male mice of Alb-Cre-Cas9Tg mice (Cre & Cre+Cas9), and 2 cohorts of n=16-20 male mice of the inducible Cre-Cas9Tg mouse lines (Cre & Cre+Cas9), the latter of which were split further into two groups each and treated with either vehicle (sunflower oil) or Tamoxifen in sunflower oil, generating the following four groups; Cre inactive (OIL), Cre+Cas9 inactive (OIL), Cre active (tamoxifen) and Cre+Cas9 active (tamoxifen). Only the final group (Cre+Cas9 active) was expected to express Cas9, with the others serving as either Cre or tamoxifen control groups.

Animal Treatments and Husbandry

All mice were bred and sourced through the ARA Precinct Animal Centre and randomly allocated into their respective groups. For tamoxifen inducible models, they were treated as follows. For ACTA1-Cre-ERT2 and AdipoQ-Cre-ERT2 models, mice were aged to 6-8 weeks old before being gavaged with either Tamoxifen (80mg/kg) in sunflower oil, or sunflower oil alone, for 3 consecutive days. For the MHC-alpha-Cre-ERT2 model, mice were

15

336   IP injected once with 40mg/kg of Tamoxifen in sunflower oil, or sunflower oil alone.

337   Following tamoxifen treatment, mice were left to recover for 2 weeks, after which they were

338   maintained on a normal chow diet (Normal rodent chow, Specialty feeds, Australia) and

339   housed at 22°C on a 12hr light/dark cycle with access to food and water *ad libitum* with cages

340   changed weekly for 12 weeks. Cohorts of mice were subjected to EchoMRI and body weight

341   analysis throughout the study period. In the last two weeks of the study period, all animals

342   underwent oral glucose tolerance tests, whilst the MHC-alpha mice were also subjected to

343   cardiac function assessment via echocardiography. At the end of the study, mice were fasted

344   for 4-6 hours and then anesthetized with a lethal dose of ketamine/xylazine before blood and

345   tissues were collected, weighed and snap frozen for subsequent analysis.

346

347   **Glucose Tolerance Tests**

348   Oral glucose tolerance tests (oGTT) were performed as previously described (Bond et al.,

349   2019a; Bond et al., 2021). In the final two weeks of the study period mice were fasted for 4-6

350   hours and gavaged at a glucose dose of 2g/kg of lean mass as determined by EchoMRI.

351   Blood glucose was determined using a glucometer at the following times points; 0, 15, 30,

352   45, 60, 90 and 120 minutes.

353

354   **EchoMRI**

355   Body composition was analyzed using the 4 in 1 NMR Body Composition Analyzer for Live

356   Small Animals, according to the recommendations of the manufacturer (EchoMRI LLC,

357   Houston, TX, USA). This provides measurements of lean mass and fat mass in living animals

358   as previously described (Bond et al., 2019a; Bond et al., 2021).

359

360   **Histology**

361 Liver and muscle were embedded cut side down in OCT before being frozen in a bath of

362 isopentane submerged in liquid nitrogen. After freezing, blocks were brought to -20°C and

363 5µm sections were cut using a Leica Cryostat. Sections were mounted and dried overnight at

364 room temperature before being fixed in Methanol. WAT samples were fixed in formalin and

365 mounted in Paraffin, before 5µm sections were cut on a Leica microtome. All sections were

366 stained with hematoxylin and eosin and slide images were captured using Olympus Slide

367 scanner VS120 (Olympus, Japan) and viewed in the supplied program (OlyVIA Build 13771,

368 Olympus, Japan).

369

370 **Quantitative PCR (qPCR)**

371 RNA was isolated from tissues using RNAzol reagent and isopropanol precipitation as

372 previously described (Bond et al., 2021; Bond et al., 2019b). Briefly, cDNA was generated

373 from RNA using MMLV reverse transcriptase (Invitrogen) according to the manufacturer's

374 instructions. qPCR was performed on 10ng of cDNA using the SYBR-green method on an

375 ABI 7500, using primer sets outlined in Table 1. Primers were designed to span exon-exon

376 junctions where possible, and were tested for specificity using BLAST (Basic Local

377 Alignment Search Tool; National Centre for Biotechnology Information). Amplification of a

378 single amplicon was estimated from melt curve analysis, ensuring only a single peak and an

379 expected temperature dissociation profile were observed. Quantification of a given gene was

380 determined by the relative mRNA level compared with control using the delta-CT method,

381 which was calculated after normalisation to the housekeeping gene *Ppia* or *Rplp0*.

382

383 **Echocardiography**

384 Echocardiography was performed on mice anaesthetised with isoflurane (1.5-2%) at the end

385 of the 12-week period following tamoxifen induction, using a 15-MHz linear transducer L15-

17

386   7io with a Philips iE33 Ultrasound Machine (North Ryde, NSW, Australia). Data were

387   analyzed and verified by two independent researchers according to QC procedures and

388   validation measures as outlined previously (Donner et al., 2018).

389

390   **Data Inclusion and Exclusion Criteria**

391   For animal experiments, phenotyping data points were excluded using the following pre-

392   determined criteria: if the animal was unwell at the time of analysis, there were identified

393   technical issues (such as unclear signal from echocardiography) or data points were identified

394   as outliers using Tukey's Outlier Detection Method (Q1 minus 1.5 IQR or Q3 plus 1.5 IQR).

395   If repeated data points from the same mouse failed QC based on pre-determined criteria, or

396   several data points were outliers as per Tukey's rule, the entire animal was excluded from

397   that given analysis (i.e. during glucose tolerance tests, indicating inappropriate gavage). For

398   in vivo and in vitro tissue and molecular analyzes, data points were only excluded if there

399   was a technical failure (i.e. poor RNA quality, failed amplification in qPCR), or the value

400   was biologically improbable. This was performed in a blinded fashion (i.e. on grouped

401   datasets before genotypes were known).

402

403

404 **Tables**

Gene	Forward primer (5' – 3')	Reverse primer (5' – 3')
Cre	AGGGCGCGAGTTGATAGCT	GAGCGATGGATTTCCGTCTCT
spCas9	CCAAGAGGAACAGCGATAAG	CACCACCAGCACAGAATAG
GFP	CAGGAGCGCACCATCTTCTT	CTTGTGCCCCAGGATGTTG
Col1a2	GGGAATGGAGCAAGACAGTCTT	TGCGATATCTATGATGGGTAGTCTCA
Chop	AGGAGCCAGGGCCAACA	TCTGGAGAGCGAGGGCTTT
Vim	GAAATTGCAGGAGGAGATGC	GGATTCCACTTTCCGTTCAA
Plin2	CCCGTATTTGAGATCCGTGT	TAGGTATTGGCAACCGCAAT
Tnfa	CCAGACCCTCACACTCAGATC	CACTTGGTGGTTTGCTACGAC
Il1b	GACGGCACACCCACCCT	AAACCGTTTTTCCATCTTCTTT
Nppa	GGGGGTAGGATTGACAGGAT	AGGGCTTAGGATCTTTTGCG
Nppb	ACAAGATAGACCGGATCGGA	AAGAGACCCAGGCAGAGTCA
Atp2a2	AATATGAGCCTGAAATGGGC	TCAGCAGGAACTTTGTCACC
Myh6	AAGATAGTGGAACGCAGGGA	CTCTTCAGCAGCGGTTTGAT
Myh7	AGCATTCTCCTGCTGTTTCC	GAGCCTTGGATTCTCAAACG
Col1a1	GGTTTCCACGTCTCACCATT	ACATGTTCAGCTTTGTGGACC
Mck	TGAGGTCTGGGTACTCCTCC	CCTCCACAGCACAGACAGAC
Tmem8c	GGAGGCCATGGTCTACCTCT	GGGCTGTTCCATAGATGCTG
Mef2c	GCCGGACAAACTCAGACATTG	GGGTTTCCCAGTGTGCTGAC
Myog	CAACCAGGAGGAGCGCGATCTCCG	AGGCGCTGTGGGAGTTGCATTCACT
Myod	AGGCCGTGGCAGCGA	GCTGTAATCCATCATGCCATCA
Cd36	TTGTACCTATACTGTGGCTAAATGAGA	CTTGTGTTTTGAACATTTCTGCTT
Cebpa	TGGACAAGAACAGCAACGAG	GTCACTGGTCAACTCCAGCA
Pparg	GTTTTATGCTGTTATGGGTG	GTAATTTCTTGTGAAGTGCTCATAG
Ucp1	ACTGCCACACCTCCAGTCATT	CTTTGCCTCACTCAGGATTGG

405

406

407 **Table 1**

408 Forward and reverse primer sets for detection of the designated mouse genes using qPCR.

409

420   **Author contributions**

421   BGD and ACC designed and conceived the study. BGD wrote the manuscript and all other

422   authors read and/or edited the manuscript. BGD, STB, DCH, AZ, CY, EAMG, YL, HK,

423   KIW and GIL performed animal experiments and phenotyping. BGD, STB, AZ, TS, YL, YF

424   and YT analyzed data, processed tissue samples and performed molecular and biochemical

425   experiments. PG, JRM, PJM and ACC provided reagents, experimental advice and access to

426   infrastructure and resources.

427

428   **Conflicts of interest**

429   The authors declare that they have no conflicts of interest.

430

431

20

432 **References**

433 Bond, S.T., Kim, J., Calkin, A.C., and Drew, B.G. (2019a). The Antioxidant Moiety of

434 MitoQ Imparts Minimal Metabolic Effects in Adipose Tissue of High Fat Fed Mice. Front

435 Physiol *10*, 543.

436 Bond, S.T., King, E.J., Henstridge, D.C., Tran, A., Moody, S.C., Yang, C., Liu, Y., Mellett,

437 N.A., Nath, A.P., Inouye, M., et al. (2021). Deletion of Trim28 in committed adipocytes

438 promotes obesity but preserves glucose tolerance. Nat Commun *12*, 74.

439 Bond, S.T., Moody, S.C., Liu, Y., Civelek, M., Villanueva, C.J., Gregorevic, P., Kingwell,

440 B.A., Hevener, A.L., Lusis, A.J., Henstridge, D.C., et al. (2019b). The E3 ligase MARCH5 is

441 a PPARgamma target gene that regulates mitochondria and metabolism in adipocytes. Am J

442 Physiol Endocrinol Metab *316*, E293-E304.

443 Broeders, M., Herrero-Hernandez, P., Ernst, M.P.T., van der Ploeg, A.T., and Pijnappel, W.

444 (2020). Sharpening the Molecular Scissors: Advances in Gene-Editing Technology. iScience

445 *23*, 100789.

446 Charlesworth, C.T., Deshpande, P.S., Dever, D.P., Camarena, J., Lemgart, V.T., Cromer,

447 M.K., Vakulskas, C.A., Collingwood, M.A., Zhang, L., Bode, N.M., et al. (2019).

448 Identification of preexisting adaptive immunity to Cas9 proteins in humans. Nat Med *25*,

449 249-254.

450 Donner, D.G., Kiriazis, H., Du, X.J., Marwick, T.H., and McMullen, J.R. (2018). Improving

451 the quality of preclinical research echocardiography: observations, training, and guidelines

452 for measurement. Am J Physiol Heart Circ Physiol *315*, H58-H70.

453 Enache, O.M., Rendo, V., Abdusamad, M., Lam, D., Davison, D., Pal, S., Currimjee, N.,

454 Hess, J., Pantel, S., Nag, A., et al. (2020). Cas9 activates the p53 pathway and selects for p53-

455 inactivating mutations. Nat Genet *52*, 662-668.

456   Fu, Y., Foden, J.A., Khayter, C., Maeder, M.L., Reyon, D., Joung, J.K., and Sander, J.D.

457   (2013). High-frequency off-target mutagenesis induced by CRISPR-Cas nucleases in human

458   cells. Nat Biotechnol *31*, 822-826.

459   Hendel, A., Fine, E.J., Bao, G., and Porteus, M.H. (2015). Quantifying on- and off-target

460   genome editing. Trends Biotechnol *33*, 132-140.

461   Laidlaw, B.J., Duan, L., Xu, Y., Vazquez, S.E., and Cyster, J.G. (2020). The transcription

462   factor Hhex cooperates with the corepressor Tle3 to promote memory B cell development.

463   Nat Immunol *21*, 1082-1093.

464   Link, R.W., Nonnemacher, M.R., Wigdahl, B., and Dampier, W. (2018). Prediction of

465   Human Immunodeficiency Virus Type 1 Subtype-Specific Off-Target Effects Arising from

466   CRISPR-Cas9 Gene Editing Therapy. CRISPR J *1*, 294-302.

467   Molla, K.A., and Yang, Y. (2019). CRISPR/Cas-Mediated Base Editing: Technical

468   Considerations and Practical Applications. Trends Biotechnol *37*, 1121-1142.

469   Platt, R.J., Chen, S., Zhou, Y., Yim, M.J., Swiech, L., Kempton, H.R., Dahlman, J.E., Parnas,

470   O., Eisenhaure, T.M., Jovanovic, M., et al. (2014). CRISPR-Cas9 knockin mice for genome

471   editing and cancer modeling. Cell *159*, 440-455.

472   Shamsi, F., Xue, R., Huang, T.L., Lundh, M., Liu, Y., Leiria, L.O., Lynes, M.D., Kempf, E.,

473   Wang, C.H., Sugimoto, S., et al. (2020). FGF6 and FGF9 regulate UCP1 expression

474   independent of brown adipogenesis. Nat Commun *11*, 1421.

475   Singh, P., Schimenti, J.C., and Bolcun-Filas, E. (2015). A mouse geneticist's practical guide

476   to CRISPR applications. Genetics *199*, 1-15.

477   Zhu, C., Jiang, Z., Xu, Y., Cai, Z.L., Jiang, Q., Xu, Y., Xue, M., Arenkiel, B.R., Wu, Q., Shu,

478   G., et al. (2020). Profound and redundant functions of arcuate neurons in obesity

479   development. Nat Metab *2*, 763-774.

480

481   **Figure Legends**

482   **Figure 1: Tissue Specific and Inducible Expression of Cas9 in four mouse models.**

483   **A.** Schematic outlining the breeding strategy and generation of the four tissue specific Cas9

484   transgenic mouse lines. The LSL-spCas9Tg mouse was bred with four different Cre-lines

485   (Albumin-Cre = Liver, AdipoQ-Cre-ERT2 = adipose, MHC-alpha-Cre-ERT2 = cardiac,

486   ACTA1-Cre/-ERT2 = skeletal muscle) to generate lines that were independently maintained

487   and studied. **B.** Relative Cre-recombinase expression as determined by qPCR for each line

488   (annotated across the bottom) in the various tissues (annotated across the top) for each mouse

489   line. Data are normalized to a housekeeping gene (*Rplp0*) and presented as arbitrary unit

490   (AU) for "Cas9+Cre Active" compared to "Cre active" groups. Adjusted expression of Cas9

491   and GFP as determined by qPCR and presented as fold change to control in the heart, liver

492   and muscle of **C.** spCas9Tg+Alb-Cre constitutively active Cre line, showing just the two

493   groups per tissue = Cre-Cas9 and Cre+Cas9 as indicated by the (+) and (-) signs at the bottom

494   of the graph, Cas9 and GFP in the **D.** spCas9Tg+MHC-alpha-Cre/-ERT2 mice, **E.**

495   spCas9Tg+ACTA1-Cre/-ERT2 mice and **F.** spCas9Tg+AdipoQ-Cre/-ERT2 mice. Because

496   the MHC-alpha-, ACTA1- and AdipoQ-Cre are inducible (tamoxifen, TAM) lines, there are

497   four groups per tissue = Cre-Cas9 (no TAM), Cre-Cas9 (plus TAM), Cre+Cas9 (no TAM)

498   and Cre+Cas9 (plus TAM) as indicated by the (+) and (-) signs at the bottom of the graphs.

499   All data are presented as mean±SEM, n=4-12/group. LSL = lox-STOP-lox, spCas9 = Cas9

500   from *S. Pyogenes*, Tg = transgenic, eGFP = enhanced green fluorescent protein, ERT2 = 2 x

501   tamoxifen sensitive mutant estrogen receptor

502

503   **Figure 2: Tissue Specific Expression of Cre-Recombinase, Cas9 and GFP does not**

504   **Impact Animal Body Weight or Tissue Weights.** All four tissue specific Cas9 mouse lines

505   were aged to approximately 18-20 weeks of age and analyzed for **A.** Body weight, **B.** Liver

23

506   weight at cull, **C.** Fat mass by EchoMRI (final two weeks), **D.** Lean mass by EchoMRI (final

507   two weeks) and **E.** heart weight at cull. The four groups per line are as follows: Cre (inactive

508   - light grey), Cre+Cas9 (inactive – dark grey), Cre (active – light blue) and Cre+Cas9 (active

509   – dark blue). All data are presented as mean±SEM, n=6-11/group. Albumin Cre-line is

510   constitutively active so the inactive groups were designated as "not inducible". ND = not

511   determined in this line.

512

513   **Figure 3: Tissue Specific Expression of Cre-Recombinase, Cas9 and GFP does not Alter**

514   **Molecular or Physiological Readouts of Tissue Function.** Molecular and functional read

515   outs of tissue function specific were performed. Alb-Cre line (liver specific) was investigated

516   for changes in **A.** hepatic mRNA expression for pathways indicative of fibrosis (*Col1a2,*

517   *Vim*), ER stress (*Chop*), lipid metabolism (*Plin2*) and inflammation (*Tnfa, Il1b*) as analyzed

518   by qPCR (n=12/group), and **B.** representative images of liver tissue morphology as assessed

519   by histology with H&E staining. The MHC-alpha-Cre-ERT2 line (cardiac specific) was

520   analyzed for changes in **C.** cardiac mRNA expression for pathways indicative of cardiac

521   pathology (*Nppa, Nppb, Atp2a2, Myh6* and *Myh7*) and fibrosis (*Col1a1*), **D.** Mass of tissues

522   pertinent to cardiac pathology (heart, atria, left ventricle (LV), right ventricle (RV), and lung)

523   and whole body animal health (spleen, kidney and liver) and **E.** measurement of heart

524   function including heart rate and fractional shortening (FS%) as analyzed by

525   echocardiography, n=6-10/group.   The ACTA1-Cre-ERT2 line (muscle specific) was

526   investigated for changes in **F.** *Tibialis anterior* (TA) mRNA expression for pathways

527   indicative of muscle maturation (*Mck*), regeneration (*Mef2c, Myod* and *Myog*) and fusion

528   (*Tmem8c*) as analyzed by qPCR, **G.** Temporal changes in lean (muscle) mass during the

529   study (at timepoints indicated on graph) as analyzed by EchoMRI and **H.** muscle (TA)

530   morphology as assessed by histology with H&E staining n=5-8/group. The AdipoQ-

24

531   Cre/ERT2 line (adipose specific) was investigated for changes in **F.** white adipose tissue

532   (WAT) gene expression for pathways indicative of lipid uptake (*Cd36*), adipocyte

533   differentiation (*Cebpa, Pparg*) inflammation (*Tnfa, Il1b*) and WAT browning (*Ucp1*) as

534   analyzed by qPCR, **G.** Temporal changes in fat (adipose) mass during the study (at

535   timepoints indicated on graph) as analyzed by EchoMRI and **H.** WAT morphology as

536   analyzed by histology with H&E staining, n=4-9/group. All data are presented as

537   mean±SEM, scale bar represents 100µm.

538

539   **Figure 4: Tissue Specific Expression of Cre-Recombinase, Cas9 and GFP does not Alter**

540   **Whole Body Glucose Homeostasis.** All four Cas9 lines were phenotyped for parameters of

541   whole body glucose homeostasis at the end of the study. This included assessment of fasting

542   blood glucose for **A.** Alb-Cre (n=11-12/group), **D.** MHC-alpha-Cre-ERT2 (n=7-10/group),

543   **G.** ACTA1-Cre-ERT2 (n=8-9/group) and **J.** AdipoQ-Cre-ERT2 (n=6-8/group) and two-hour

544   glucose tolerance as performed by oral glucose tolerance tests (oGTT) on **B.** Alb-Cre **E.**

545   MHC-alpha-Cre-ERT2 **H.** ACTA1-Cre-ERT2 and **K.** AdipoQ-Cre-ERT2 mice as quantified

546   by 90 minute cumulative area under the curve (AUC) analysis for **C.** Alb-Cre **F.** MHC-alpha-

547   Cre-ERT2 **I.** ACTA1-Cre-ERT2 and **L.** AdipoQ-Cre-ERT2. All data are presented as
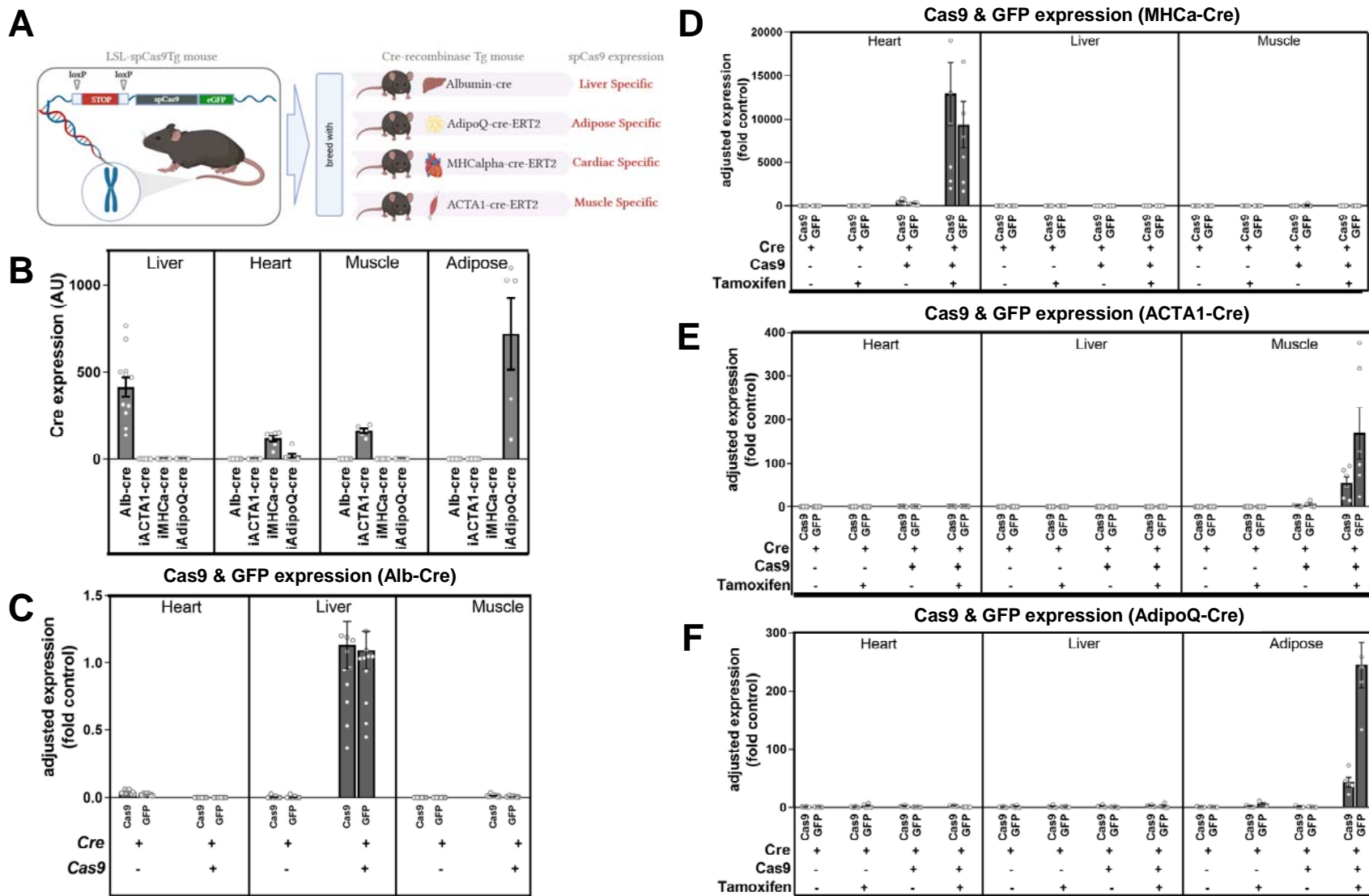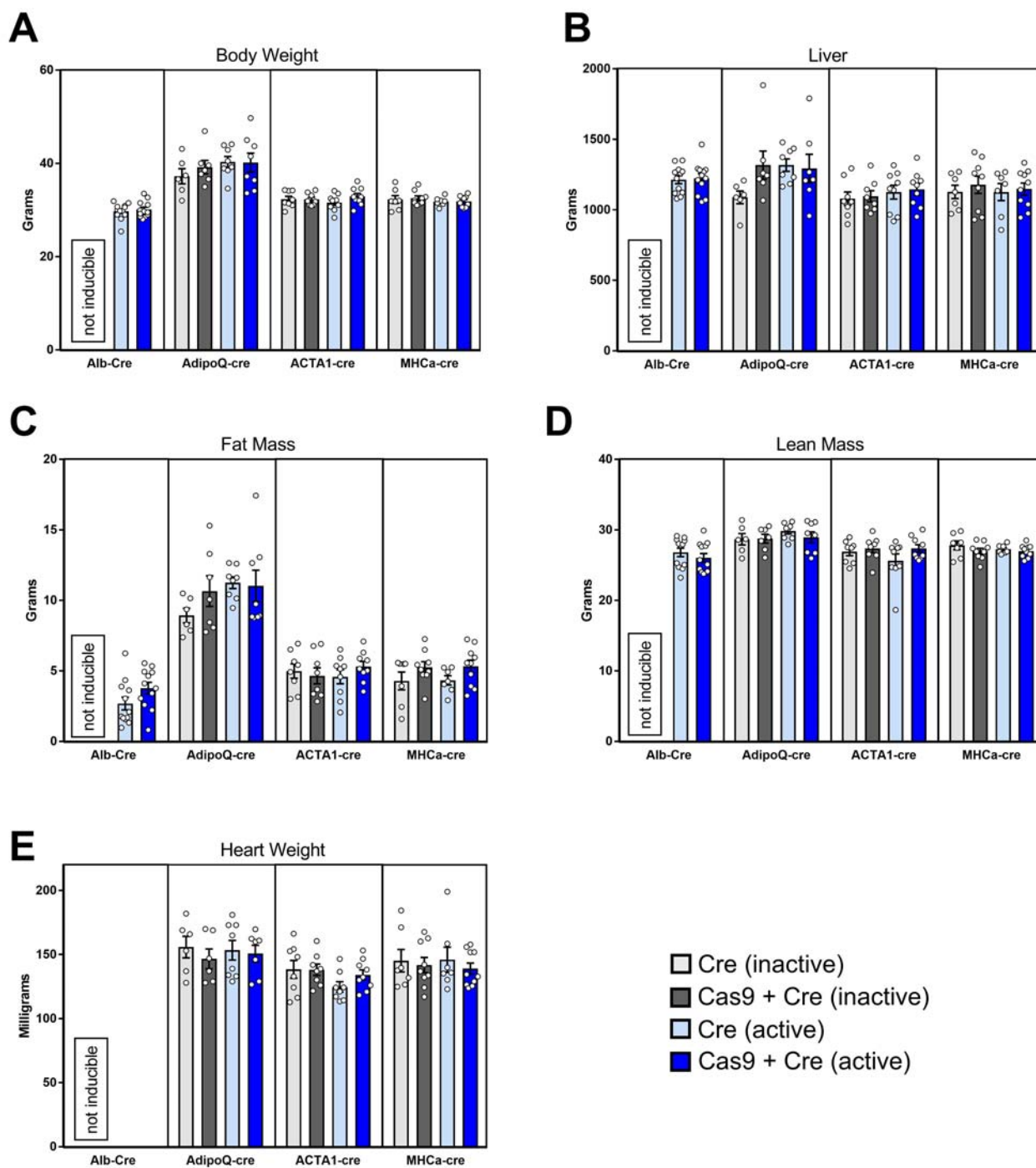
548   mean±SEM.

549

Figure 1

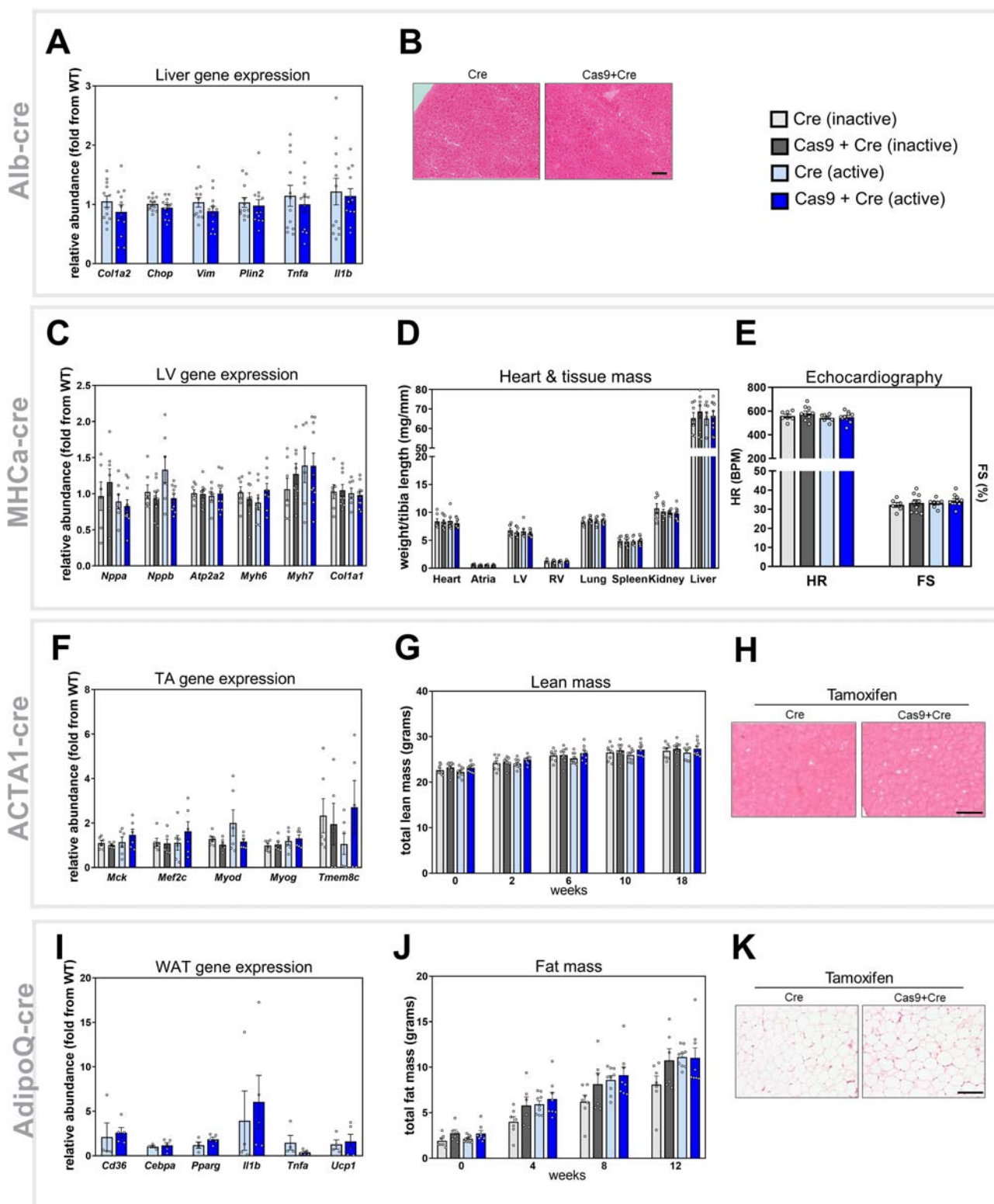**Figure 2**

Figure 3

Figure 4